Reduced Simulations for High-Energy Physics, a Middle Ground for Data-Driven Physics Research

Uraz Odyurt$^{1,2[0000-0003-1094-0234]}$, Stephen Nicholas Swatman$^{3,4[0000-0002-3747-3229]}$, Ana-Lucia Varbanescu$^{3,5[0000-0002-4932-1900]}$, and Sascha Caron$^{1,2[0000-0003-2941-2829]}$

[1] High-Energy Physics, Radboud University, Nijmegen, The Netherlands
[2] National Institute for Subatomic Physics (Nikhef), Amsterdam, The Netherlands
`{uodyurt,scaron}@nikhef.nl`
[3] Informatics Institute, University of Amsterdam, Amsterdam, The Netherlands
`s.n.swatman@uva.nl`
[4] European Organisation for Nuclear Research (CERN), Geneva, Switzerland
[5] CAES, University of Twente, Enschede, The Netherlands
`a.l.varbanescu@utwente.nl`

Abstract. Subatomic particle track reconstruction (tracking) is a vital task in High-Energy Physics experiments. Tracking is exceptionally computationally challenging and fielded solutions, relying on traditional algorithms, do not scale linearly. Machine Learning (ML) assisted solutions are a promising answer. We argue that a complexity-reduced problem description and the data representing it, will facilitate the solution exploration workflow. We provide the REDuced VIrtual Detector (REDVID) as a complexity-reduced detector model and particle collision event simulator combo. REDVID is intended as a simulation-in-the-loop, to both generate synthetic data efficiently and to simplify the challenge of ML model design. The fully parametric nature of our tool, with regards to system-level configuration, while in contrast to physics-accurate simulations, allows for the generation of simplified data for research and education, at different levels. Resulting from the reduced complexity, we showcase the computational efficiency of REDVID by providing the computational cost figures for a multitude of simulation benchmarks. As a simulation and a generative tool for ML-assisted solution design, REDVID is highly flexible, reusable and open-source. Reference data sets generated with REDVID are publicly available. Data generated using REDVID has enabled rapid development of multiple novel ML model designs, which is currently ongoing.

Keywords: Reduced-order modelling, Simulation, High-energy physics, Synthetic data

1 Introduction

In many computational sciences, the adoption of ML-assisted solutions can lead to serious gains in computational efficiency and data processing capacity, resulting from algorithmic advantages intrinsic to ML. Computational efficiency can also be achieved by paving the way for the utilisation of dedicated hardware, i.e., GPUs, FPGAs and purpose-built accelerators. ML algorithms are highly compatible with the use of such specialised hardware. In this work, we explore the use of ML-assisted techniques in high-energy physics.

ML-assisted solution design is an explorative and data-demanding endeavour. One of the effective approaches to achieve a suitable design is Design-Space Exploration (DSE). Complex problems involve many parameters, contributing to a space with many dimensions, which in turn deems the exploration expensive. There is often a need for simplification of the problem domain, i.e., search-space reduction, to facilitate the initial steps within this explorative process.

Generative elements are often needed as part of the explorative process, to enable synthetic data generation in large quantities, at will. Furthermore, designing and training models with better rigour requires total control over all aspects of data generation. Providing sufficient control and on demand ability to synthesise data that is representative of corner cases contributes to achieving effective models. Such corner cases seldom/disproportionally appear in real-world data or highly accurate, i.e., *physics-accurate*, simulation data.

Use-case Our focus is a major use-case from the field of High-Energy Physics (HEP), *the critical task of subatomic particle track reconstruction (tracking)*, present in data processing for experiments performed at the Large Hadron Collider (LHC). Detectors such as ATLAS, record interaction data of subatomic particles with detector sensors, allowing physicists to reconstruct particle trajectories through tracking algorithms and to gain knowledge on how subatomic particles behave. Current solutions rely largely on traditional, computationally expensive statistical algorithms, with Kalman filtering as their most demanding block. Even with constant efforts channelled into better parallelisation schemes for these algorithms, the data consumption capability is rather limited. The challenge will be even greater with the upcoming High-Luminosity LHC upgrade [3], given its increased data volume generation and experiment frequency.

Although physics-accurate simulators, such as Geant4 [1], are readily available, applying such levels of accuracy to generative elements comes at a hefty computational cost. Accordingly, these simulators are not suitable for frequent *timely* executions and constant data generation, as required for DSE iterations. As such, we propose an exploration methodology that can be much faster, through the informed simplification of the design-space for the ML-assisted solution. Our methodology is specifically being considered for the tracking use-case. To this end, we have *designed and implemented* the *REDuced VIrtual Detector (REDVID)*, to both simplify the problem at hand and act as an efficient tool for frequent simulations and synthetic data generation. While our tool is not a fully physics-accurate one, it does respect the high-level relations present in subatomic particle collision events and detector interactions. REDVID is fully (re)configurable, allowing definition of experiments through varying detector models, while preserving the *cascading effects* of every change.

Considering possible complexity reduction strategies, the spectrum varies from physics-accurate data manipulations, e.g., dimensionality/granularity reduction, to omitting the scenario interactions beforehand. A strategy solely based on data reduction will fail to preserve the behavioural integrity of the system, as it will fail to propagate cascading effects resulting from reductions. Even simplified examples such as the TrackML data [2] are too complex.

Contribution REDVID, as an experiment-independent, fully (re)configurable, and complexity-reduced simulation framework for HEP [20], is provided. Simulations consist of complexity-reduced detector models, alongside a particle collision event simulator with reduced behavioural-space. REDVID is intended as a simulation-in-the-loop for ML model design workflows, providing:

– ML model design - Problem simplification facilitates ML solution design, as opposed to real-world use-case definitions, which are often too complex to negotiate directly.
– Parametric flexibility - The model generator is capable of spawning detectors based on reconfigurable geometries.
– Computational efficiency - Behavioural-space reductions directly improve event simulation and processing times.

Our other contributions include:

– Supporting pedagogical tasks in higher education by presenting complex interactions from HEP experiments through understandable data.
– Publishing open reference data sets, which are of independent interest for physicists and data scientists alike [21, 18].

Outline Section 2 provides the background on HEP experiments and similar simulators. In Section 3, we provide the design details considered for REDVID. Notable implementation techniques are elaborated in Section 4. Data set related results are given in Section 5, followed by Sections 6 and 7, covering the relevant literature and our conclusions, respectively.

2 Background and motivation

In this section we elaborate the premise of HEP experiments, as well as the role of simulation in these, to get familiar with the context of our use-case.

2.1 HEP experiments

When talking about *HEP experiments*, we refer to high-energy particle collision events. Two types of collision experiments are performed at LHC: proton-proton and ion-ion collisions. Protons are extracted from hydrogen atoms, while ions are actually heavy lead ions. Beams of particles are sent down the beam pipe in opposing directions and made to collide at four specific spots. These four spots are the residing points of the four major detectors installed at LHC, namely, ALICE [9], ATLAS [10], CMS [11] and LHCb [12].

Take the ATLAS detector for instance. The role played by ATLAS in the study of fundamental particles and their interactions, rely on two main tasks, *tracking* and *calorimetry*. Through tracking, i.e., particle track reconstruction, the momentum, p, of a particle can be calculated, while the energy, E, is calculated through calorimetry. Having the momentum and the energy for a given particle, its mass, m, can be determined, following the *energy-momentum relation* expressed as,

$$E^2 = (mc^2)^2 + (pc)^2 .$$

In the above equation, c represents the speed of light and is a constant. The mass measurement allows the study of the properties for known particles, as well as potentially discovering new unknown ones. As such, it is fair to state that *particle track reconstruction is one of the major tasks in high-energy physics*.

2.2 Role of simulation in HEP

Simulation allows for, amongst others, the validation and training of particle track reconstruction algorithms. Two distinguished stages are considered for HEP event simulations, i.e., *physics event generation* and *detector response simulation* [15]. Event generation as the first stage, involves the simulation of particle collision events, encompassing the processes involved in the initial proton-proton or ion-ion interactions. Event generation is governed by intricate sets of physical rules and is performed by software packages such as Herwig [13] and Pythia [23], i.e., physics-accurate simulations.

Detector response simulation, the second stage, integrates the movement of the particles generated by the first stage through a detector geometry, simulating the decay of unstable particles, the interactions between particles and matter, electromagnetic effects, and further physical processes such as hadronisation. Common event simulators providing such functionality include Geant4 [1], FLUKA [5] and MCNP [16]. In accelerator physics applications, event simulators are used to simulate the interactions between particles and sensitive surfaces in an experiment, as well as with so-called passive material, such as support beams. Interactions with sensitive surfaces may undergo an additional *digitisation* step, simulating the digital signals that can be read out of the experiment. Considering the example of ATLAS, three data generating simulators are notable, namely, Geant4, FATRAS [15] and ATLFAST [22].

Following the Monte Carlo simulation approach, FATRAS has been designed to be a fast simulator. It is capable of trajectory building based on a simplified reconstruction geometry and does provide support for material effects, as well as particle decay. FATRAS also generates hit data.

ATLFAST follows a different approach towards trajectory simulation and doesn't generate hit data, making it unsuitable for tracking studies. ATLFAST relies on hard-coded smearing functions based on statistics from full simulations. These functions are dependent on particle types, momentum ranges and vertex radii. Such details are specific to the design elements of the virtual detector geometry. A change in the design will require finding new functions.

REDVID fills the gap for a reconfigurable framework, suitable for first-phase solution exploration and design. This is due to the deliberate reduction in complexity, for both the generated data and the problem description, while keeping the high-level causal relations in place. REDVID is end-to-end parametric, i.e., all the generated data is built upon the detector geometry and randomised particle trajectories, both reconfigurable. REDVID has been developed in Python, making its integration with Python-based ML design workflows seamless. Figure 1 positions REDVID versus other well-known tools, as we consider it.

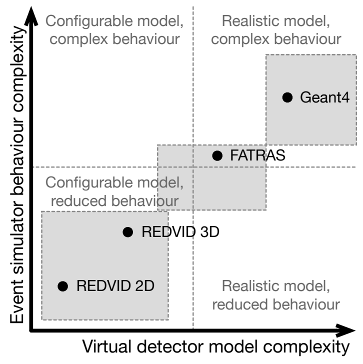
Configurable model, complex behaviour
Realistic model, complex behaviour
Geant4
FATRAS
Configurable model, reduced behaviour
REDVID 3D
REDVID 2D
Realistic model, reduced behaviour
Event simulator behaviour complexity
Virtual detector model complexity

Fig. 1: Different simulators are capable of providing different levels of complexity, depicted as grey areas. ATLFAST is not included for lack of hit data generation.

3 Simulation application and design

The underlying question here is what is a good strategy for designing and training a capable and rigorous ML model to predict the behaviour of a (complex) real system? For our HEP use-case, the system is already complex; and when considering the upcoming High-Luminosity LHC upgrade [3], this complexity will increase even further. As such, when looking for an ML-assisted solution for tracking, we need to efficiently explore a large set of options.

Addressing complex real-world tasks directly will require synthesising close to real-world data, which can be performed by high-accuracy simulations. High-accuracy simulations in general, and physics-accurate simulations in particular, are extremely expensive computational tasks. Having such tools as part of an exploration workflow, e.g., ML model design, triggering frequent executions of the simulation with altered configuration, will inevitably turn into a serious challenge. Even if there are accommodating hardware resources available, algorithmic limitations will turn software tools into workflow bottlenecks. Yet another notable drawback is the high cost of energy when running frequent computationally expensive tasks. To alleviate this massive challenge, it is highly beneficial, and perhaps necessary, to not only design reduced models and simulators[6], but *to provide parametric (re)configurability to support automated exploration.*

[6] A model and a simulator go hand in hand to form a simulation.

However, the initial testing of new ML-assisted solutions, i.e., ML model designs, does not require the ground truth, which physics-accurate simulations are designed to produce. Instead, we argue that a cost-effective and reduced simulation, preserving the behavioural relations of the complex system (proton-proton/ion-ion collision event experiments), can be better and more effectively integrated in ML model design workflows, as shown in Figure 2.

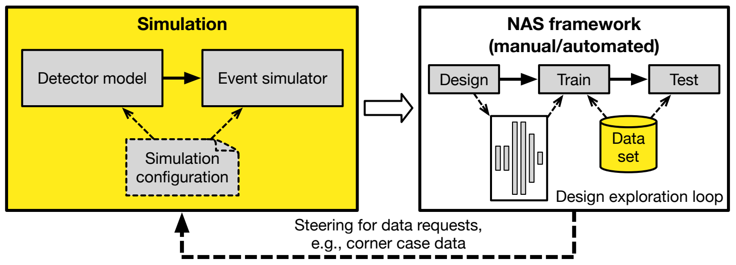

Fig. 2: Reduced simulations in ML model design workflows, e.g., a Neural Architecture Search (NAS), with this paper's focus on the area with the yellow fill.

3.1 Reduction approach

Having a validly approximate representation is achieved through the reduction of the behavioural-space to a minimal subset, best encapsulating the complex system. Both model complexity and simulator complexity can be targets of such a reduction. The first and foremost effect of an approximate simulation is better computational efficiency. Note that there can be many such approximations, depending on the intended balance between computational efficiency and behavioural approximation level. The other advantage, especially when it comes to ML model design processes, is facilitation of an effective model design by providing a middle ground that has a lower complexity and can be used for better understanding of the challenge and testing of the early designs.

Both actual experiments and physics-accurate simulations for our use-case, i.e., proton-proton/ion-ion collision events inside a detector such as ATLAS, are immensely complex. Removing (some of) the physics-accurate constraints results in major behavioural-space reductions. This applies to both the detector model and the behaviour affecting the event simulator. While moving away from physics-accuracy, our aim has been to conserve logical, mathematical and geometrical relations, which would provide the basis for a flexible parameterisation. Preserving relations between interacting elements of a system preserves occurrence of *cascading effects* when the system is being steered through reconfiguration. For instance, a change in the structural definition of the detector model will affect the recorded hit points during the event simulation. It must be noted that we have intentionally avoided the time dimension complexities. Accordingly, a list of major reductions that we have considered follows.

– Simplified detector geometry: Compared to the real detector, we have considered much simpler elements for the geometry of our virtual detector

model, consisting of elements with disk or cylinder shapes, ultimately arriving at a Reduced-Order Model (ROM).
- Particle types: Currently, we do not consider explicit particle types in our event simulator. The track type variation however, could be seen as a consequence of differing particle types.
- Simplified tracks: Currently, we consider particles traversing a linear (straight), helical uniform, or helical expanding paths. Helical tracks could be seen as the effect of a magnetic field on charged particles.
- Collision points: The real experiments involve multiple collisions happening almost at the same time. We consider a single event at the origin for linear tracks and a non-aligning one for helical tracks, i.e., origin smearing.
- Hit coordinates smearing: We introduce noise in our hit calculations and hit coordinate parameters by drawing random samples from a Gaussian distribution. We also consider the noise standard deviation as proportional to the variable range. The noise ratio can be adjusted by the user.

3.2 Detector model

At its core, a detector model is comprised of the geometric definitions of the included elements, shapes, sizes, and placements in space. Although we can support a variety of detector geometries, the overall structure, especially for our experimental results, is based on the ATLAS detector. Accordingly, there are four sub-detector types, *Pixel*, *Short-strip*, *Long-strip* and *Barrel*. The pixel and the barrel types have cylindrical shapes with the pixel being a filled cylinder, while the barrel being a cylinder shell with open caps. These are not hard requirements, as the geometry is fully parametric, and differing definitions can be opted for, e.g., a pixel as a cylinder shell. The long-strip and the short-strip types are primarily intended as flat disks, but can be defined as having a thickness, rendering them as cylinders. Sub-detector types can be selectively present or absent. Figure 3 depicts a representative variation of the detector geometry involving the aforementioned elements.

Structurally speaking, in a real-world detector, like ATLAS, the internals of short-strip and long-strip sub-detector types are different. We on the other hand, reduce such complexities to placement location and size, i.e., distance from the origin and sub-detector disk radius. Note that our geometric model does support disk thickness, which basically would turn disks into shallow cylinders. However, we have considered flat disks for our experiments.

3.3 Particle collision event simulation

One of the simplifications for our complexity reduction approach is to consider a single collision per event. However, the list of complexities, even without the polluting effects of multiple collisions, is extensive. Particles travelling through the detector matter could lead to secondary collisions, resulting in drastic changes in their trajectory. Such secondary collisions could also lead to the release of particles not originating from the collision event itself. These will show up as

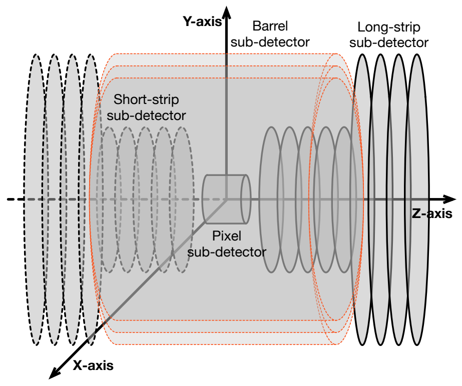

Fig. 3: Parametric detector geometry, allowing for inclusion/exclusion of different sub-detector types, with full control over sub-layer counts, sizes and placements.

tracks with unusual starting points within the detector space. Some particles could also come to a halt, which would be seen as abruptly terminating tracks.

Such physics-accurate behaviour of particles interacting with the present matter in detectors is not considered for our simulator. It must be noted that the generation of tracks originating far away from the origin and prematurely terminating tracks, can be emulated in our simulator in a randomised fashion.

4 Implementation

Though both two-dimensional (2D) and three-dimensional (3D) spaces are supported, we will focus on the implementation details relevant to the 3D case. REDVID is open source [19] and has been developed in Python.

4.1 Modules

Considering the tasks at hand, detector spawning and event simulation, our software can be divided into three main logical modules: *Detector generator*, *Event simulator* and *Reporting*, depicted in Figure 4. The current implementation considers the sequential execution of modules in the order given. However, one can easily generate detectors without simulating events, or simulate events with previously generated detectors, or even calculate hits based on previously generated tracks. Such input/output capability will allow our software to interact with other commonly utilised tools. The main configuration parameter defining the execution path is the `detector_type`, which can be 2D or 3D.

4.2 Coordinate systems

We have opted for the cylindrical coordinate system to represent sub-detectors, tracks and hits. This is convenient, as we are considering the Z-axis as the beam

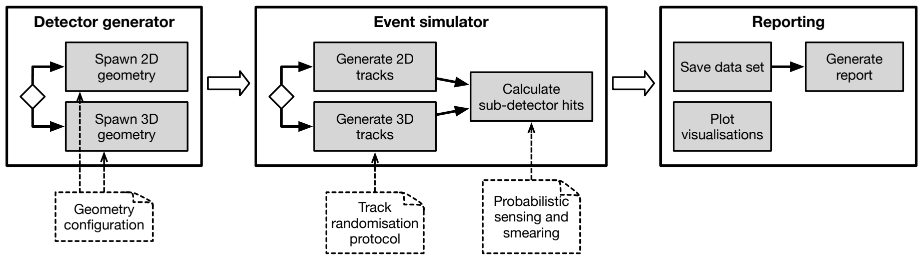

Fig. 4: REDVID modules, including a detector model generator, an event simulator, generating randomised tracks and calculating sub-detector hit points based on tracks and geometric data, as well as different reporting elements.

pipe in LHC experiments and all geometric shapes defined within a detector, whether disks or cylinders, are actually of the type cylinder. The three parameters to define any point in the cylindrical coordinate system are the radial distance from the Z-axis, the azimuthal angle between the X-axis and the radius, and the height of the point from the XY-plane, i.e., r, θ and z, respectively.

In this coordinate system, hit points can be precisely defined given the tuple $(r_{hit}, \theta_{hit}, z_{hit})$. Geometric shapes can also be defined with boundaries for r_{sd} and z_{sd}, e.g., a disk will have fixed z_{sd}, unbounded θ and bounded r_{sd}. Here *sd* stands for sub-detector. Our software does support partial disks, i.e., a disk with a hole in the middle, which can be considered when the beam pipe is expected to be part of the geometry. Disks with thickness (cylinders) will have a small boundary for the parameter z_{sd}. As previously explained, short-strip and long-strip sub-detector types are defined as disks. For the pixel type, as it is a filled cylinder, both r_{sd} and z_{sd} will be bounded. When it comes to the barrel type, as it is a cylinder shell, there will be a fixed r_{sd} with bounded z_{sd}.

To implement linear tracks and to define them in the cylindrical coordinate system, both a direction vector and a point, P_0, that the track (line) goes through are needed. The direction vector, V_d, is considered as a vector from the origin, landing on a point in space, represented with a tuple (r_d, θ_d, z_d). The direction vector is randomised and then normalised for the z parameter, meaning that the direction vector will either have $z_d = 1$ or $z_d = -1$. The boundaries of this randomisation depend on the track randomisation protocol, explained in the next section. If we consider all linear tracks as starting from the detector origin, the point $(0, 0, 0)$ is considered on the track. However, this is rarely the case. The resulting parametric form of a track (line) is,

$$\begin{aligned} r &= r_0 + t \cdot r_d \,, \\ \theta &= \theta_0 + \theta_d \,, \\ z &= z_0 + t \cdot z_d \,, \end{aligned}$$

with (r, θ, z) representing a point on the track, (r_0, θ_0, z_0) as the origin point, $\langle r_d, \theta_d, z_d \rangle$ as the direction vector, and t as free variable. Similarly, the parametric form for helical track definitions is,

$$\begin{aligned} r &= r_0 + a \cdot t\,, \\ \theta &= \theta_0 + d \cdot t\,, \\ z &= z_0 + b \cdot t\,, \end{aligned}$$

with (r, θ, z) representing a point on the track and (r_0, θ_0, z_0) as the origin point, while a, d and b represent radial, azimuthal and pitch coefficients, respectively.

Regarding both linear and helical tracks, our software supports origin smearing, i.e., the starting point of helical tracks is in a randomised vicinity of the point $(0, 0, 0)$.

4.3 Track randomisation protocols

As seen in Figure 4, the track randomisation step directly affects sub-detector hit calculation and is totally dependent on the randomisation protocol indicated in the configuration. Focusing on the implementation for the 3D space, different track randomisation protocols can be considered. We list four base protocols and five combination protocols, mixing the characteristics of base protocols:

Protocol 1 - Last layer hit guarantee Hits are guaranteed to occur on the farthest layer of every sub-detector type, which means the farthest layer of every sub-detector type is the randomisation domain for the landing points of tracks. A hit guarantee on the last layer will also guarantee hits on the previous layers for that sub-detector type. This protocol is designed to maximise the number of hits per sub-detector type within the data set.

In principle, our implementation applies *Protocol 1* per each available sub-detector type and randomly selects from the total generated track pool. Since for instance, if a track lands on the last layer of strip sub-detector types, it might not necessarily result in hit points on barrel layers.

Protocol 2 - Spherically uniform distribution To have a more uniform distribution of randomised tracks, without imposing any geometric conditions, is to have the track end points land on a sphere. Note that tracks do not have actual end points as these are unbounded lines.

Protocol 3 - Conical jet simulation Tracks are randomised in distinct subsets, bundled in a close vicinity within a narrow cone, representing a jet(s). This protocol on its own may not be a sensible choice and it would work best in combination with other protocols.

Protocol 4 - Beam pipe concentration Tracks have a higher concentration around the beam pipe, i.e., higher track generation probability as the radius gets smaller.

Without giving exhaustive and repetitive descriptions, feasible combination protocols are: *Protocols 1 and 3*, *Protocols 1 and 4*, *Protocols 2 and 3*, *Protocols 3 and 4* and *Protocols 1, 3 and 4*.

For data generation we have only considered protocol 1 to increase recorded hit points for all tracks and to have hit points for all sub-detector types. Additional track randomisation protocols focusing on specific corner cases, can be easily defined and added to the tool. To implement protocol 1, i.e., to guarantee that tracks land on the last layer of a sub-detector type, we consider the coordinate domain of the last layer as the randomisation domain for track direction vectors. Thus, before normalisation, all randomised V_d will land on the last layer.

Not every combination is allowed. For instance, protocols 1 and 2 cannot be applied at the same time, as it is self-evident that a spherical uniform distribution and a last layer hit guarantee cannot be true at the same time. Accordingly, we can consider the base protocols within two main categories, *distribution protocols*, affecting how tracks are distributed in space, and *feature protocols*, defining special forms of localised distribution. Currently, protocol 3 is the only feature protocol defined. While feature protocols can be combined with any distribution protocol, most distribution protocols are mutually exclusive. A combination of two or more base distribution protocols will also lead to another, more specific, distribution protocol, e.g., protocols 1 and 4. Figure 5 provides a visual overview.

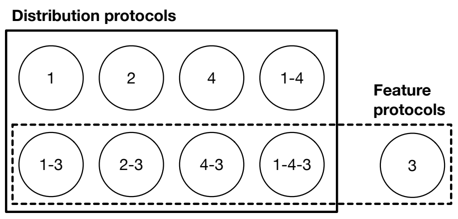

Fig. 5: Visualising how different base distribution and feature protocols can be combined to achieve more complex track randomisation behaviour.

4.4 Hit point calculation

Regarding hit point coordinates, i.e., $(r_{hit}, \theta_{hit}, z_{hit})$, depending on the sub-detector shape, we are dealing with either a fixed z_{sd} or a fixed r_{sd}, for disks and barrels, respectively. Here, we consider the disks as being flat and to have no thickness, while the barrels consist only of cylinder shells. Shapes with thickness are supported, for which the techniques involved will be similar.

Considering the set of track equations, we are to calculate the free variable t at the sub-detector layer of interest, i.e., t_{sd}. For hit coordinates at disks,

$$\begin{aligned} z_{hit} &= z_{sd}\,, \\ \theta_{hit} &= \theta_d\,, \\ t_{sd} &= \frac{z_{sd}}{z_d} = \frac{z_{sd}}{1}\,, \\ &\Rightarrow t_{sd} = z_{sd}\,, \\ r_{hit} &= t_{sd} \cdot r_d = z_{sd} \cdot r_d\,. \end{aligned}$$

Note that in the above calculation z_d and z_{sd} must have matching signs, rendering $t_{sd} > 0$. In other words, tracks extruding towards the positive or the negative side of the Z-axis can hit sub-detector layers present at the positive or the negative side of the Z-axis, respectively. We also know that $z_d \neq 0$.

A similar calculation considering the r_{sd} as fixed will result in the hit coordinates for a barrel sub-detector layer, which we will not repeat here. General approach towards calculation of hits resulting from helical tracks follows the same principles, which we will not repeat here. Figure 6 depicts a simple event with five tracks, including separate views of the full event (Figure 6a) and calculated hits (Figure 6b), for demonstration purposes. Note that the detector orientation is vertical.

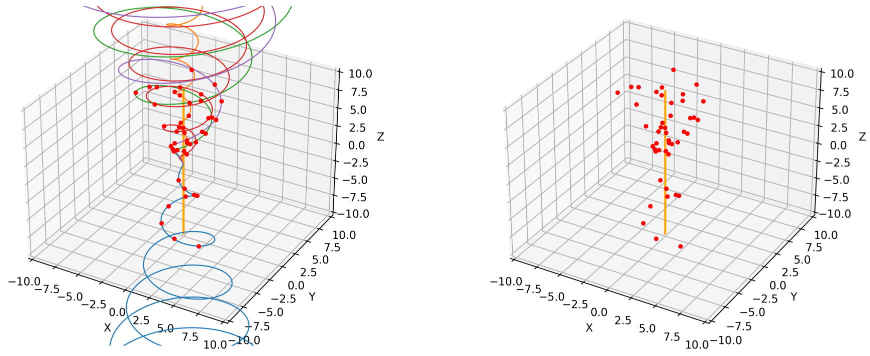

(a) The full view of this event (b) The hits view of this event

Fig. 6: An example event with five tracks

5 Data set generation

We have followed simulation recipes with 10 000 events and varying track counts of [1, 10 000] per event for each experiment, for both linear and helical tracks. Hit recording is performed with smearing enabled and the detector geometry is the same for all recipes. These generated data sets for linear and helical tracks are intended as reference for physicists and data scientists alike and are publicly accessible over Zenodo open repository [21, 18]. Data set schema alongside data header descriptions are included in the accompanying `README` files.

In order to evaluate the performance of REDVID, we have benchmarked the execution of simulations with a lower event count, 1 000 events per simulation and similar variations of track concentrations per event as before, i.e., [1, 10 000]. For our metric collections, including CPU-time and execution duration, high-precision counters from the `time` library available in Python have been used. The collected CPU-time results are provided in Table 1.

Simulations have been performed on the DAS-6 compute cluster [4]. The machines used are each equipped with a single 24-core AMD EPYC 7402P processor and 128 GB of main memory. Note that the mean CPU-time calculations

Table 1: REDVID execution CPU-time cost for simulations of 1 000 events with various track concentrations. All values are in milliseconds. Full simulation times are provided in minutes as well.

Track(s) per event	**3D detector spawning**	**Track randomisation Mean**	**Hit discovery Mean**	**Full simulation 1 000 events (minutes)**
1	0.025	0.043	1.463	2 731.17 (0.05)
10	0.025	0.083	13.429	15 418.589 (0.26)
100	0.025	0.465	129.864	137 623.954 (2.29)
1 000	0.025	4.582	1 285.989	1 353 396.641 (22.56)
10 000	0.024	43.765	12 496.208	13 591 628.526 (226.53)

do not include the first event of each recipe batch. This is due to the presence of cold-start effect for the first event and delays resulting from it.

Though we have enforced single-threaded operation for our benchmarks, workload parallelisation is rather trivial. The number of events to be generated can be divided into any desired number of batches and distributed amongst multiple threads. Considering the timing results, we observe that the CPU-time values scale linearly, i.e., a tenfold increase in the track concentration per event results in roughly a tenfold increase in the full simulation CPU-time.

6 Related work

While the overall available data is abundant, corner case data is rather scarce. Real-world data, or data synthesised with accurate (in our case physics-accurate) simulations is complex in terms of data dimensionality and granularity. This complexity is directly resulting from the complexity of the real system, or the accurate model of the system in case of simulations. Within the HEP landscape, we touched upon the complexity of simulators such as Geant4 in Section 2, as well as the dependence on these simulators by tools like ATLFAST.

The first challenge, lack of annotated data for one or more specific scenarios, has been recognised in the literature [14]. The second challenge though, the issue of complexity, is not as well known. A closely related acknowledgement has been made regarding the complexity level of models for simulations [8].

The two main shortcomings of the previous efforts towards the use of ML in physics problems have been use-case specificity [24] and the lack of user-friendly tools [6]. As noted by Willard et al. [24], the efforts surrounding the use of ML for physics-specific problems are focused on sub-topics, or even use-cases. Although our methodology and synthetic data focuses on the domain of tracking for detector data, we could claim that it is independent of the chosen detector.

The point from [24] regarding the computational efficiency of ROMs matches our motivation. Where our work differs is in the placement of our ROM within our methodology. Our reduced model of a detector is considered as the model for simulations aimed at synthetic data, which is different than ML-based surrogate models as ROMs [7, 17], or ML-based surrogate models built from ROMs [25].

7 Conclusion and future work

With many computational science applications exploring the use of ML-assisted solutions, there is a need for reduced complexity simulations to facilitate the design process. We show how such a reduction through ROMs and a smaller behavioural-space for the simulator, can result in a lower complexity for synthesised data. This is particularly relevant for our HEP use-case.

We have presented the design and implementation details of REDVID (REDuced VIrtual Detector), our simulation framework fulfilling such a reduction. To demonstrate REDVID's feasibility, we executed it with relevant workload recipes, and have made available the resulting data sets over Zenodo open repository. We further analysed the computational cost figures for these experiments, and we conclude that, even though our tool is developed in Python, computational cost figures (case in point, 15 seconds, 138 seconds and 22 minutes of CPU-time for 1 000 events with 10, 100 and 1 000 tracks per event, respectively) indicate efficiency for frequent executions. Accordingly, the lightweight nature of REDVID simulations makes our tool a suitable choice as a simulation-in-the-loop with data-driven workflows for HEP, e.g., searching for a ML-assisted solution to address the challenge of tracking.

We have explained that, to opt for such an approximation, is a deliberate act, positioning REDVID as a suitable middle ground amongst other available tools, not as exact as physics-accurate simulations, and not as synthetic as dummy data generators. The reduced complexity especially allows for early problem formulation and testing at early stages, when dealing with ML-assisted solution design workflows. Yet another advantage of reduced complexity data that still respects the high-level relations, is in its pedagogical merit, enabling problem solving practices in higher education.

Acknowledgments. This project is supported by the Nederlandse Organisatie voor Wetenschappelijk Onderzoek (NWO), a.k.a., the Dutch Research Council (grant no. 62004546).

References

1. Agostinelli, S. *et al.*: Geant4—a simulation toolkit. Nuclear Instruments and Methods in Physics Research Section A: Accelerators, Spectrometers, Detectors and Associated Equipment (2003)
2. Amrouche, S. *et al.*: The Tracking Machine Learning Challenge: Accuracy Phase. In: The NeurIPS '18 Competition (2020)
3. Apollinari, G., Brüning, O., Rossi, L.: High Luminosity LHC Project Description. Tech. rep., CERN (2014)
4. Bal, H. *et al.*: A Medium-Scale Distributed System for Computer Science Research: Infrastructure for the Long Term. Computer (2016)

5. Böhlen, T. *et al.*: The FLUKA Code: Developments and Challenges for High Energy and Medical Applications. Nuclear Data Sheets (2014)
6. Carleo, G. *et al.*: Machine learning and the physical sciences. Rev. Mod. Phys. (2019)
7. Chen, G., Zuo, Y., Sun, J., Li, Y.: Support-Vector-Machine-Based Reduced-Order Model for Limit Cycle Oscillation Prediction of Nonlinear Aeroelastic System. Mathematical Problems in Engineering (2012)
8. Chwif, L., Barretto, M., Paul, R.: On simulation model complexity. In: 2000 Winter Simulation Conference Proceedings (Cat. No.00CH37165) (2000)
9. Collaboration, T.A. *et al.*: The ALICE experiment at the CERN LHC. Journal of Instrumentation
10. Collaboration, T.A. *et al.*: The ATLAS Experiment at the CERN Large Hadron Collider. Journal of Instrumentation (2008)
11. Collaboration, T.C. *et al.*: The CMS experiment at the CERN LHC. Journal of Instrumentation (2008)
12. Collaboration, T.L. *et al.*: The LHCb Detector at the LHC. Journal of Instrumentation (2008)
13. Corcella, G. *et al.*: HERWIG 6: an event generator for hadron emission reactions with interfering gluons (including supersymmetric processes). Journal of High Energy Physics (2001)
14. de Melo, C.M. *et al.*: Next-generation deep learning based on simulators and synthetic data. Trends in Cognitive Sciences (2022)
15. Edmonds, K. *et al.*: The Fast ATLAS Track Simulation (FATRAS). Tech. rep., CERN (2008)
16. Forster, R. *et al.*: MCNP™ Version 5. Nuclear Instruments and Methods in Physics Research Section B: Beam Interactions with Materials and Atoms (2004)
17. Kasim, M.F. *et al.*: Building high accuracy emulators for scientific simulations with deep neural architecture search. Machine Learning: Science and Technology (2021)
18. Odyurt, U.: *REDVID Collision Event Data – Helical Tracks and Hits*. Zenodo, 2024. `https://doi.org/10.5281/zenodo.10514246`.
19. Odyurt, U.: REDVID Repository, (2023). `https://VirtualDetector.com/redvid/repository.html`
20. Odyurt, U.: REDVID Simulation Framework, (2023). `https://VirtualDetector.com/redvid/`
21. Odyurt, U., Swatman, S.N.: *REDVID Collision Event Data – Linear Tracks and Hits*. Zenodo, 2023. `https://doi.org/10.5281/zenodo.8322302`.
22. Richter-Was, E., Froidevaux, D., Poggioli, L.: ATLFAST 2.0 a fast simulation package for ATLAS. Tech. rep., CERN (1998)
23. Sjöstrand, T., Mrenna, S., Skands, P.: PYTHIA 6.4 physics and manual. Journal of High Energy Physics (2006)
24. Willard, J., Jia, X., Xu, S., Steinbach, M., Kumar, V.: Integrating Scientific Knowledge with Machine Learning for Engineering and Environmental Systems. ACM Comput. Surv. (2022)
25. Xiao, D. *et al.*: A reduced order model for turbulent flows in the urban environment using machine learning. Building and Environment (2019)